

Self-assembled nanowhiskers grown by MBE on InP(001) surface

Alexei Bouravlev^{*,1,2}, Kazuyuki Minami¹, Takayuki Ishibashi¹, and Katsuaki Sato¹

¹ Graduate School of Engineering, Tokyo University of Agriculture and Technology, 184-8588 Tokyo, Japan

² A. F. Ioffe Physico-Technical Institute, 194021 St. Petersburg, Russian

Received 23 February 2006, revised 6 April 2006, accepted 26 June 2006

Published online 31 August 2006

PACS 75.75.+a, 81.07.Vb, 81.15.Hi, 81.16.Dn

Ge and MnP nanowhiskers were synthesized by molecular-beam epitaxy technique on InP(001) surface concurrently. The growth of Ge nanowhiskers is found to be assisted by Mn-based nanocluster-mediated vapour-liquid-solid mechanism of growth, whereas the growth of MnP nanowhiskers seems to be caused by catalyst-free mechanism. Magnetic property measurements revealed that samples with prevailing Ge nanowhiskers exhibit ferromagnetic behaviour up to room temperature.

© 2006 WILEY-VCH Verlag GmbH & Co. KGaA, Weinheim

1 Introduction

One-dimensional nanostructures such as nanorods, nanotubes, nanowhiskers have attracted much attention due to their potential application in nanoscale devices [1–5]. The standard techniques for its fabrication based on lithography techniques often have the disadvantage concerning with insufficient quality of technological processes. Therefore methods based on the self-assembled growth of nanostructures, such as bottom-up fabrication of nanowhiskers are a major focus of interest for the creation of novel nanodevices [2–6]. Among them a vapour-liquid-solid (VLS) growth proposed in the 1960 by Wagner and Ellis is noteworthy [7]. According to this method, the formation of the nanowhiskers occurs due to the adsorption of the gas-phase reactants by liquid droplets that are formed from nanosized metal clusters [6]. The sizes and the positions of nanowhiskers depend directly on the diameters of the metal clusters. However, nanowhiskers can be contaminated due to the presence of the impurity metal on their tips. As a consequence alternative techniques for the growth of nanowhiskers, which do not require any catalyst, also are of importance for the technological aspects of nanoelectronics [8, 9].

The magnetic self-assembled nanowhiskers deserve special attention because their fabrication makes possible to tune the Curie temperature, remanent magnetization and coercive saturation field by means of the control over their sizes, shapes and distributions that in turn allows us to utilize such materials not only for data storage and nanoscale spintronics applications, but also for the investigation of the fundamental magnetic properties of low-dimensional structures. Recently Mn-doped nanowhiskers have been successfully synthesized using different methods [10–14]. Mn-doped ZnO and GaN nanowhiskers exhibiting ferromagnetic behaviour were prepared by vapour-phase evaporation [10] and chemical vapour deposition (CVD) [11], respectively. The similar magnetic properties have been shown by Mn⁺ ion im-

* Corresponding author: e-mail: alexei@cc.tuat.ac.jp, Phone: +81 42 388 74 32, Fax: +81 42 388 74 32

planted ZnO nanowhiskers [12]. Mn-doped CdS and ZnS nanowhiskers have been fabricated using a core/shell methodology [13]. Furthermore, MnP nanorods were synthesized via thermal decomposition of continuously delivered metal-phosphine complexes [14].

In this paper, we report on the molecular beam epitaxial growth and the characterization of MnP and Ge self-assembled nanowhiskers on the InP(001) substrates.

2 Methods

Self-assembled (SA) nanowhiskers have been grown by conventional molecular beam epitaxy (MBE) on InP(001) substrate using Knudsen cells for the Mn and Ge evaporation as well as cracking cell for the decomposition of tertiarybutylphosphine (TBP) into P_2 flux. The “epi-ready” InP(100) wafers were annealed at 480 °C in vacuum inside a treatment chamber in a P_2 flow for 20 minutes. The duration of growth ranged from 30 minutes up to 2 hours at the temperatures between 430–545 °C which were controlled using a temperature controller and an infrared pyrometer. The beam flux of Mn was adjusted in the range between $0.5 - 0.9 \times 10^{-8}$ Torr and that of Ge in the range between $0.9 - 1.5 \times 10^{-8}$ Torr using an ion gauge. The flow rate of TBP gas was set at 2.0 sccm by using a mass flow controller, whereas the temperature of the cracking cell was kept in the range of 810 – 835 °C to assure efficient decomposition of TBP into P_2 during the MBE growth. The growth process was monitored using in-situ reflection high energy electron diffraction (RHEED) measurements.

The morphology and microstructure of nanowhiskers were examined by scanning electron microscope (SEM, Hitachi S-4500) and scanning transmission electron microscope (STEM, FEI TECNAI-F20). Chemical compositions were measured using an energy-dispersive X-ray analysis (EDX) attached to the SEM and STEM apparatus. The crystals were analyzed by X-ray diffraction technique using an X-ray diffractometer (XRD, Philips X'Pert type). Temperature and magnetic-field dependences of magnetization were measured by a superconducting quantum interference device (SQUID) and vibration sample (VSM, TOEI VSM-5-19) magnetometers.

3 Results and discussion

3.1 Growth and structure of self-assembled nanowhiskers

The fabrication of self-assembled nanowhiskers was made possible by the development of the technology of MnGeP₂ thin film growth [15, 16], that is chalcopyrite-type ternary compound [15–17].

Contrary to usual above-mentioned metal catalyst vapour-liquid-solid (VLS) growth [3, 7], in our experiments we did not use any preliminary tailor-made metal catalyst layer. SA nanowhiskers were grown directly on InP(001) surface by MBE.

Figures 1a–d demonstrate a scanning electron microscopy images of SA nanowhiskers grown at different temperatures on InP(001) surface. At low temperatures around 435 °C the nanowhiskers with typical diameters close to 20 nm and length up to 2 μm which are spaced at different intervals can be obtained (Fig. 1a and b). These individual SA nanowhiskers have preferential direction which corresponds to the $\langle 111 \rangle$ crystallographic orientation and seems to be dependent on the crystallographic form and the orientation of the host substrate. Unfortunately, we cannot control the exact position of individual nanowhiskers on the surface unlike the positions of nanowhiskers prepared according VLS growth mechanism, since they can be preassigned by the distribution of preliminary fabricated nanosized metal cluster. In spite of the fact, that individual nanowhiskers have a small dispersion in diameters, they differ greatly in lengths which appear to be dependent on the time of growth. On further increasing the growth temperature the microstructure and the distribution of nanowhiskers can be considerably modified (Fig. 1c and d). Instead of widely distributed individual nanowhiskers, the arrays of SA nanowhiskers that have random (Fig. 1c) or at higher temperatures solid (Fig. 1d) distribution on the InP(001) surface and different shape with or without precipitated nanoclusters can be obtained.

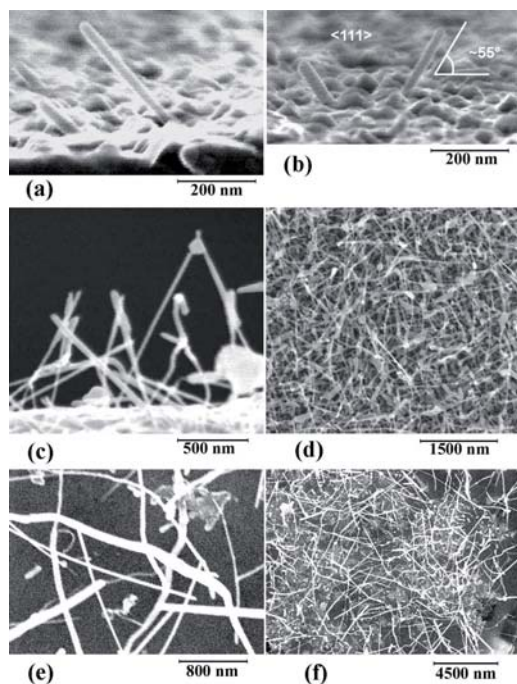


Fig. 1 SEM images of individual (a), (b) and arrays of SA nanowiskers (c), (d) as well as MnP nanowiskers (e), (f) grown on InP(001) surface. The temperature of the growth: (a), (b) 435 °C; (c) 500 °C; (d) 520 °C; (e), (f) 545 °C.

The phases of the samples with SA nanowiskers were firstly identified by XRD analysis (Fig. 2). X-ray diffraction θ - 2θ scan data of the samples showed few dominant peaks inherent to all samples. First of them, the broad amorphous-like peak at $2\theta \sim 24^\circ$ is a contribution from the glass plate used as a sample holder. The peaks at $2\theta \sim 30.5^\circ$ and $2\theta \sim 63.4^\circ$ bear on 002 and 004 diffraction of InP substrates, respectively. The diffraction peak observed at $2\theta \sim 66.04^\circ$ may be assigned to the reflection from $\text{MnGeP}_2(008)$ [15, 16]. Other peaks, which seem to be related to the MnP 111, MnP 202 and MnP 121

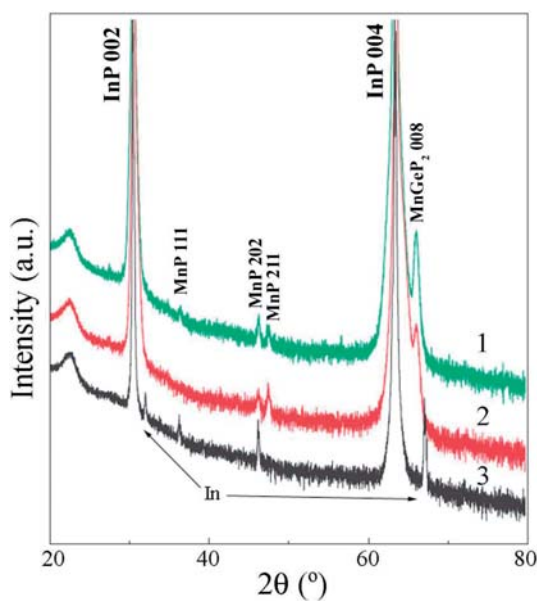


Fig. 2 X-ray diffraction pattern of samples with SA nanowiskers grown at 435 °C (1) (see Fig. 1a and b); 520 °C (2) (see Fig. 1d) and MnP nanowiskers grown at 545 °C (3).

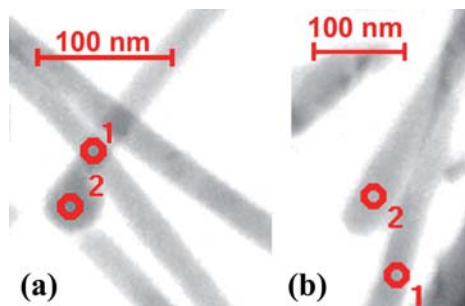


Fig. 3 Low-resolution STEM images of Ge (a) and MnP (b) nanowhiskers grown at 500 °C (see Fig. 1c). (EDX analysis of the nanowhiskers has been performed for the depicted points).

were also detected. At elevated temperatures the signal most likely assigned to MnP 111 became extinct thereby indicating that this peak can be result of the reflection from MnP nanowhiskers.

In order to verify this supposition, we have performed the growth of MnP nanowhiskers by the same above-described technique but without using Ge K-cell. The nanowhiskers obtained are shown on Fig. 1e and f. They have lengths up to 6 μm and larger dispersion in sizes. Furthermore, they are similar in structure to individual nanowhiskers grown at low temperatures, because they do not have any terminated nanocluster, as opposed to the SA nanowhiskers grown at higher temperatures. From these facts it transpires that the growth of MnP nanowhiskers is apt to be caused by non-catalytic growth mechanism which has not been thoroughly investigated [8, 9]. XRD diffraction pattern of the sample with MnP is presented on Fig. 2. Diffraction peaks that may be related to MnP 111 and MnP 202 have been also found and in doing so they substantiated our supposition. However, it should be noted, that the growth of nanowhiskers can be accompanied by the growth of thin film. In this connection some of these peaks may be assigned not only to nanowhiskers but also to the different phases of thin film.

Therefore, we have performed TEM and EDX study of the samples. For these investigations nanowhiskers were transferred from the host substrate onto Cu TEM grid. Energy dispersive X-ray analysis showed that two different types of nanowhiskers can be obtained concurrently: Ge nanowhiskers (Fig. 3a) and MnP nanowhiskers with atomic ratio Mn:P $\sim 65:20\%$ (Fig. 3b points 1 and 2).

In as much as the amount of Ge nanowhiskers at high temperatures is more than MnP as well as taking into account the XRD data, the formation of MnP nanowhiskers seems to be dominated at low temperatures (Fig. 1a and b), whereas that of Ge nanowhiskers prevails at high temperatures (Fig. 1c and d). In

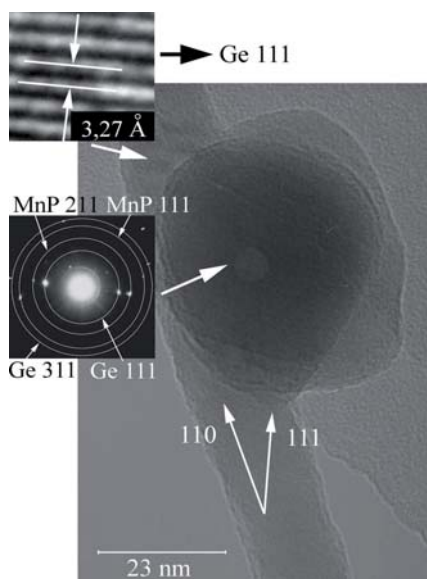


Fig. 4 TEM image of Ge nanowhisker with Mn-based nanocluster. Insets: HRTEM image of Ge nanowhiskers and the diffraction pattern of Mn-based nanocluster.

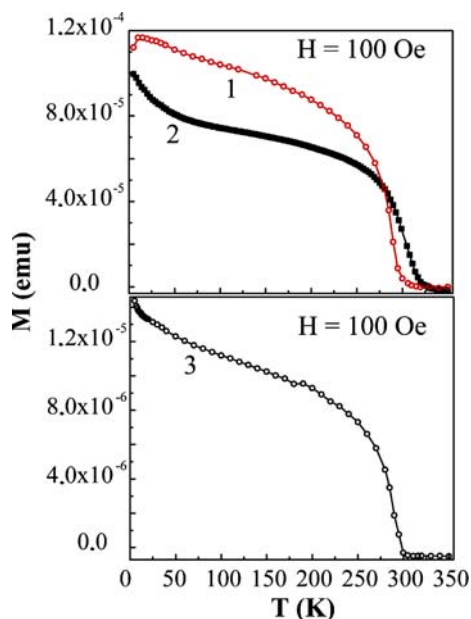


Fig. 5 (online colour at: www.pss-a.com) Temperature dependence of magnetization measured with an applied field of 100 Oe for (1) the sample with SA nanowhiskers grown at 520 °C (Fig. 1d); (2) MnGeP₂ thin film grown on GaAs(001) substrate with Ge buffer layer [16] and (3) SA nanowhiskers grown at 520 °C peeled off from the InP(001) substrate.

turn, despite the fact that we did not use an tailor-made catalyst compound, the growth of Ge nanowhiskers is found to be amenable to VLS mechanism of growth [6, 7]. The role of the catalyst for the growth in this case plays Mn-based nanoclusters with atomic composition of elements close to Mn:P:Ge 78:5:6% (Fig. 3a point 2 and Fig. 4) which seem to be self-assembled at an initial stage of the growth. TEM as well as SEM analysis has shown that most of Ge nanowhiskers are straight and uniform in diameters along their length. High-resolution TEM image demonstrated on Fig. 4 indicates that Ge nanowhiskers are single crystalline with lattice fringe spacing 0.327 nm which corresponds to (111) plane. As a consequence the Ge nanowhiskers are found to be grown along $\langle 110 \rangle$ crystallographic axis (Fig. 4).

3.2 Magnetic properties

Since the major contribution to the magnetic properties of the sample with the individual SA nanowhiskers grown at low temperatures seems to result from MnGeP₂ thin film [16] most attention has been concentrated on the investigation of samples grown at high temperatures, that is, the samples with prevailing concentration of Ge nanowhiskers (Fig. 1c and d). The measurements of the temperature and magnetic

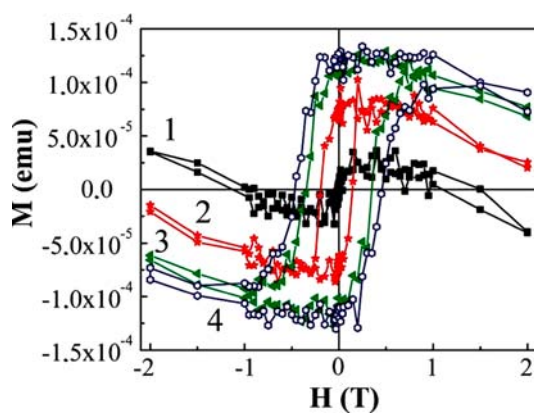


Fig. 6 (online colour at: www.pss-a.com) Hysteresis loops for the sample with SA nanowhiskers grown at 520 °C (Fig. 1d) measured at different temperatures: (1) 295 K; (2) 70 K; (3) 30 K; (4) 5 K.

Table 1 Potential second phases that can be formed during the growth of SA nanowhiskers.

phase	nature of magnetism	applicable magnetic temperature (K)	ref.
Mn	antiferromagnetic	100	12
MnO	antiferromagnetic	122	12
MnO ₂	antiferromagnetic	84	12
Mn ₃ O ₄	ferromagnetic	1443	12
MnP	ferromagnetic	291	18
MnP	antiferromagnetic	50	18
Mn ₃ P	antiferromagnetic	115	18
Mn ₂ P	antiferromagnetic	103	18
Mn _x Ge _{1-x}	ferromagnetic	25–116	19
Mn ₅ Ge ₃	ferromagnetic	296	20,21
MnGeP ₂	ferromagnetic	320	17

field dependences of magnetization have been carried out using SQUID magnetometer for both SA nanowhiskers on InP substrates and nanowhiskers which have been peeled off from wafers (Figs. 5 and 6). The magnetization of sample with SA nanowhiskers is observed to exhibit ferromagnetic behaviour up to room temperature (Fig. 5, curves 1) therewith the field dependences of magnetisation reveal hysteresis loops with coercive fields H_c are equal to 100 Oe and 4560 Oe measured at 295 K and 5 K, respectively (Fig. 6). Besides, the SA nanowhiskers peeled off from the host substrate exhibits the same ferromagnetic behaviour (Fig. 5, curves 3). Table 1 demonstrates the potential secondary phases that could form during the growth process. According to these data, ferromagnetic properties of the samples are attributable to the existence of MnGeP₂, MnP or Mn₅Ge₃ phases, but SA nanowhiskers exhibit behaviour of magnetisation that is distinct from that of MnGeP₂ thin film [16] (Fig. 5, curves 1). Therefore ferromagnetic properties of SA nanowhiskers may be caused by most likely the presence of Mn₅Ge₃ phase [21] and yet we have to take into account that MnP can also be responsible for this behaviour, in spite of the fact that magnetic properties of MnP nanowhiskers demonstrated in [14] differ from it.

4 Conclusion

We have grown self-assembled Ge and MnP nanowhiskers by molecular-beam epitaxy technique on InP(001) surface. It has been shown, that the growth of Ge nanowhiskers was appeared to be assisted by Mn-based nanocluster-mediated VLS mechanism of growth, whereas the growth of MnP nanowhiskers seemed to be caused by catalyst-free mechanism. Hence, new method for the creation of nanowhiskers with using Mn-based nanocluster as a catalyst is found. The investigation of the magnetic properties revealed that samples with prevailing Ge nanowhiskers exhibit ferromagnetic behaviour up to room temperature. Although the nature of this ferromagnetism is still an open question that requires an additional clarification such structures would be expected to exhibit the size-dependend magnetic properties which are of particular interest for nanometer scale spintronics applications.

Acknowledgements This work has been supported by 21st Century COE Program “Future Nano-Materials” of TUAT, Japanese Society for Promotion of Science (Grant P 06112 and Grant-in-Aid for Scientific Research B 17360009) and Inter-University Cooperative Research Program of Tohoku University. We sincerely thank S.Mitani from Tohoku University, H. Sosiati and N. Kuwano from Kyushu University for their help in measurements.

References

- [1] R. S. Friedman et al., Nature **434**, 1085 (2005).
- [2] G.-C. Yi et al., Semicond. Sci. Technol. **20**, S22 (2005).

- [3] L. Samuelson et al., *Physica E* **21**, 560 (2004).
- [4] S. S. Mao et al., *Int. J. Nanotechnol.* **1**, 42 (2004).
- [5] Y. Xia et al., *Adv. Mater.* **15**, 353 (2003).
- [6] K. Hiruma et al., *Appl. Phys. Lett.* **77**, 447 (1995).
- [7] R. S. Wagner and W. C. Ellis, *Appl. Phys. Lett.* **5**, 89 (1964).
- [8] A. Sekar et al., *J. Cryst. Growth* **277**, 471 (2005).
- [9] W. I. Park et al., *Adv. Mater.* **14**, 1841 (2002).
- [10] Y. Q. Chang et al., *Appl. Phys. Lett.* **83**, 4020 (2003).
- [11] D. S. Han et al., *Appl. Phys. Lett.* **86**, 032506 (2005).
- [12] K. Ip et al., *J. Vac. Sci. Technol. B* **21**, 1476 (2003).
- [13] P. V. Radovanovic et al., *Nano Lett.* **5**, 1407 (2005).
- [14] J. Park et al., *J. Am. Chem. Soc.* **127**, 8433 (2005).
- [15] K. Minami et al., *Jpn. J. Appl. Phys.* **44**, L265 (2005).
- [16] K. Sato et al., *J. Phys. Chem. Solids* **66**, 2030 (2005).
- [17] S. Cho et al., *Solid State Commun.* **129**, 609 (2004).
- [18] S. J. Pearton et al., *Mater. Sci. Eng. R Rep.* **40**, 137 (2003).
- [19] Y. D. Park et al., *Science* **295**, 651 (2002).
- [20] C. Zeng et al., *Appl. Phys. Lett.* **83**, 5002 (2003).
- [21] R. P. Panguluri et al., *phys. stat. sol. (b)* **242**, R67 (2005).